Chapter 7. Fourier Transform Infrared Spectroscopy

The thermal analysis experiments described in Chapter 5 provide insight into a number of aspects of the crystallization and melting behavior of the ethylene/α-olefin copolymers. It is inferred from the results of the cooling rate dependence of crystallinity, and from the trends observed in the cooling and subsequent heating traces, that there are two distinct regions of crystallization in these copolymers - a cooling rate-independent, reversible region at low temperatures, and a cooling rate-dependent hysteretic region at high temperatures. It is further concluded that the crystals formed during the secondary crystallization of the copolymers (studied by following the temporal evolution of the low endotherm at different crystallization temperatures) are much thinner and possess smaller lateral dimensions than the chain-folded lamellar crystals formed at higher temperatures. The preliminary model proposed indicates the involvement of two vastly different crystallization mechanisms, leading to two correspondingly different morphologies, for these copolymers. In accordance with the results of the thermal analysis studies, the AFM experiments revealed the continuous gradation in the morphology of the samples with increasing branch contents. The micrographs obtained clearly indicate that the thickness as well as the lateral dimensions of the lamellae decreases systematically with increasing comonomer concentrations. The presence of bridge-like structures between the lamellae and approximately perpendicular to their surfaces was also discerned, from the micrographs of some of the samples. It was suggested that these bridge-like features could be identified with the "fringed-micelle"-like bundled crystals introduced in Chapter 5. These crystals originate from shorter ethylene sequences present in a highly constrained amorphous phase. Furthermore, significant stresses are built up at the crystal/liquid interface in the absence of adjacent re-entry chain folding in the primary lamellae. Therefore, the secondary crystals formed under such high degrees of constraint should be less perfect than the usual orthorhombic-type crystals. These crystals may adopt a distorted orthorhombic unit cell structure[1] and may even adopt a crystal structure different from the orthorhombic form (most likely the hexagonal or monoclinic unit cell type). This aspect is investigated in the present study by performing a series of

experiments using Fourier Transform Infrared Spectroscopy (FTIR). This technique is particularly useful for the issues addressed in the present study, for the following reason. The orthorhombic crystal structure is characterized by two chains per unit cell and thereby results in a doublet in the rocking region. On the other hand, the monoclinic/hexagonal crystal forms are comprised of only one chain per unit cell and thereby yield only a singlet in the rocking region of the infrared spectrum. Therefore, the presence/absence of crystals with these two unit cell structures can be easily discerned from the infrared spectra (the rocking region is used in this study) of the samples. In this chapter, the results of the infrared experiments are reported and further correlations are drawn between the crystallization mechanism, morphology and crystal structure in the copolymers.

7.1 Infrared Spectroscopy Measurements

Fourier Transform Infrared Spectroscopy (FTIR) is a technique that is widely employed for problems concerning the structure of polymers[2,3,4]. In particular, the transmission method was adopted in the present study on copolymers. It was mentioned in Chapter 2 that the transmission method requires that the samples be completely uniform and thin enough to transmit light and to exhibit absorbance values of less than one. This requirement implies that the sample thicknesses must not exceed the range 10 to 100 μm, depending on the molar absorptivity of the groups present in the polymer of interest. In addition, the samples should be free from holes and other imperfections as well as from gradations in thickness. Accordingly, thin films of approximately 30 to 50 μm were used in the current study. It is very important to obtain films of this thickness, since thicker films may result in very high absorbances and saturation of the signal. Thinner films would lead to difficulties associated with film deformation and tackiness, especially for the higher branched materials. The details of sample preparation were discussed in detail in Chapter 3 of this dissertation.

The infrared experiments were carried out with all the ethylene/1-butene copolymers; however, they were not repeated for the ethylene/1-pentene and ethylene/1-

hexene copolymers since it has already been demonstrated unambiguously via thermal analysis studies that these three types of copolymers behave in an identical manner with regard to their crystallization and melting behaviors.

7.2 Analysis of Infrared Spectra - The Amorphous (Melt) Spectrum

The first step in the analysis of the infrared spectra was the identification of the fact that there is a significant influence of temperature, on the shape of the spectrum associated with the amorphous fraction. This is depicted in Figure 1 for EB-883 (~ 13 mole % 1-butene). It is seen from this figure that there is a noticeable decrease in the peak height of the 720cm^{-1} band with increasing temperature in the melt.

7.2.1 Modeling the Melt Spectra

The foremost objectives of the present infrared study were:

(a) to determine the presence (or absence) of a second crystal structure co-existing with the orthorhombic form, in the ethylene/α-olefin copolymers
(b) to estimate their degrees of crystallinity, and
(c) to calculate the relative contributions of crystals with the two types of unit cell structures (if there are two types) to the total absorbance.

In order to achieve these goals, it was first necessary to accurately estimate the integrated intensity and shape of the amorphous band in a sample spectrum at a given temperature. Subsequently, the amorphous band was subtracted from the infrared spectrum of the semicrystalline sample. The band representing the amorphous fraction present in a copolymer at any temperature was derived starting from the melt spectra. (The details of the method adopted are presented below).

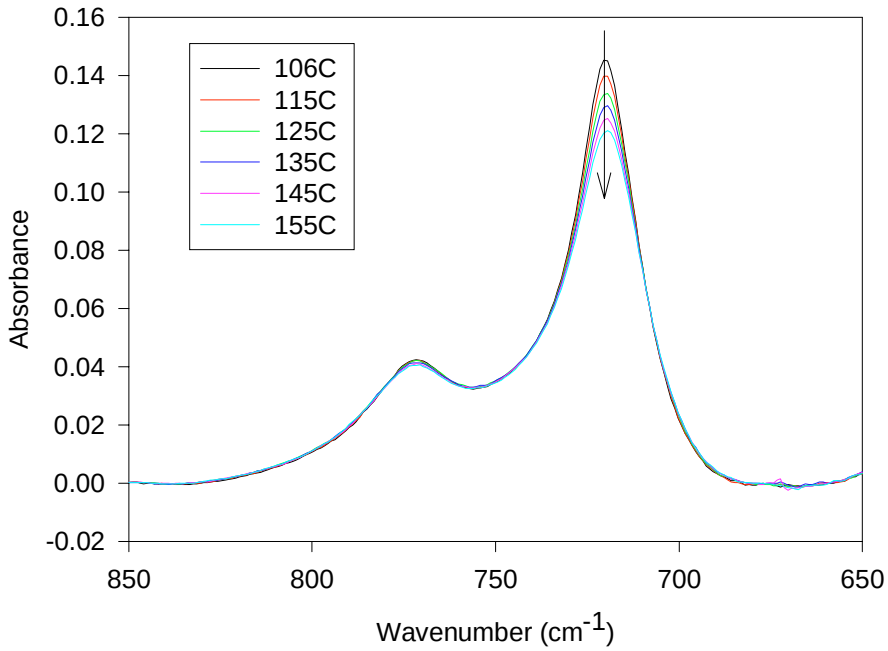

Figure 1 Influence of temperature on the infrared spectrum of EB-883 (~ 13 mole % 1-butene) (Arrow indicates increasing temperature)

However, it is clearly seen from Figure 1 that the shapes and the integrated intensities of these (melt) spectra vary considerably with temperature. Therefore, it was necessary to model this temperature dependence, in order to accurately estimate the amorphous band in the semicrystalline sample spectrum and thereby, the degree of crystallinity of the sample, at any temperature. Such a modeling was done by means of a curve-fitting procedure that is discussed below. Mathematical modeling using curve fitting is a powerful technique that can be employed to extract information of the sort that may not be possible via other direct measurements. However, it could be easily misused if proper constraints are not placed on the number and nature of the parameters employed, and could lead to a misrepresentation of the actual results. Necessary precautions were taken in this study to avoid such misuse. The procedure adopted is described below.

First, the number of peaks to be used was identified by examining the sample spectrum in the melt. A minimum of two peaks was necessary to match the two bands appearing in the melt spectra - one centered at 720cm^{-1} and the other at 775 cm^{-1}. It may be recalled from the discussion in Chapter 2 that the band at 720 cm^{-1} is associated with the -CH_2 vibrations in the rocking mode. The second band centered at 775 cm^{-1} is characteristic of the vibrations of the ethyl side branch also in the rocking mode, and is unique to ethylene/1-butene copolymers.

As a first step, a number of curve modifications were tried on a trial and error basis to determine the best curve shape that matched the band at 775cm^{-1}. The best fit was achieved when an Exponentially Modified Gaussian (EMG) curve form was used. Its mathematical representation is given below.

(1) $$y = \frac{a_0}{2a_3}\exp\left(\frac{a_2^2}{2a_3^2} + \frac{a_1 - x}{a_3}\right)\left[1 + erf\left[\frac{\sqrt{2}}{2}\left(\frac{x - a_1}{a_2} - \frac{a_2}{a_3}\right)\right]\right]$$

where a_0 = the area of the peak

a_1 = the peak position

a_2 = the peak width, and

a_3 = the peak dispersion (ratio of width to height)

This band at 775 cm^{-1} was found to remain invariant with temperature for a given branch content. However, its position as well as its integrated intensity vary as a function of branch concentration, as shown in Figure 2. Then, for a given comonomer content, the infrared spectrum of an ethylene/1-butene copolymer with the 775 cm^{-1} band subtracted out must be similar to the sample spectrum of say, an ethylene/1-octene copolymer in which the 775 cm^{-1} band is absent. Accordingly, an investigation similar to the present study was performed on a series of ethylene/1-octene copolymers in our laboratory[5], and the same conclusions were arrived at from both studies.

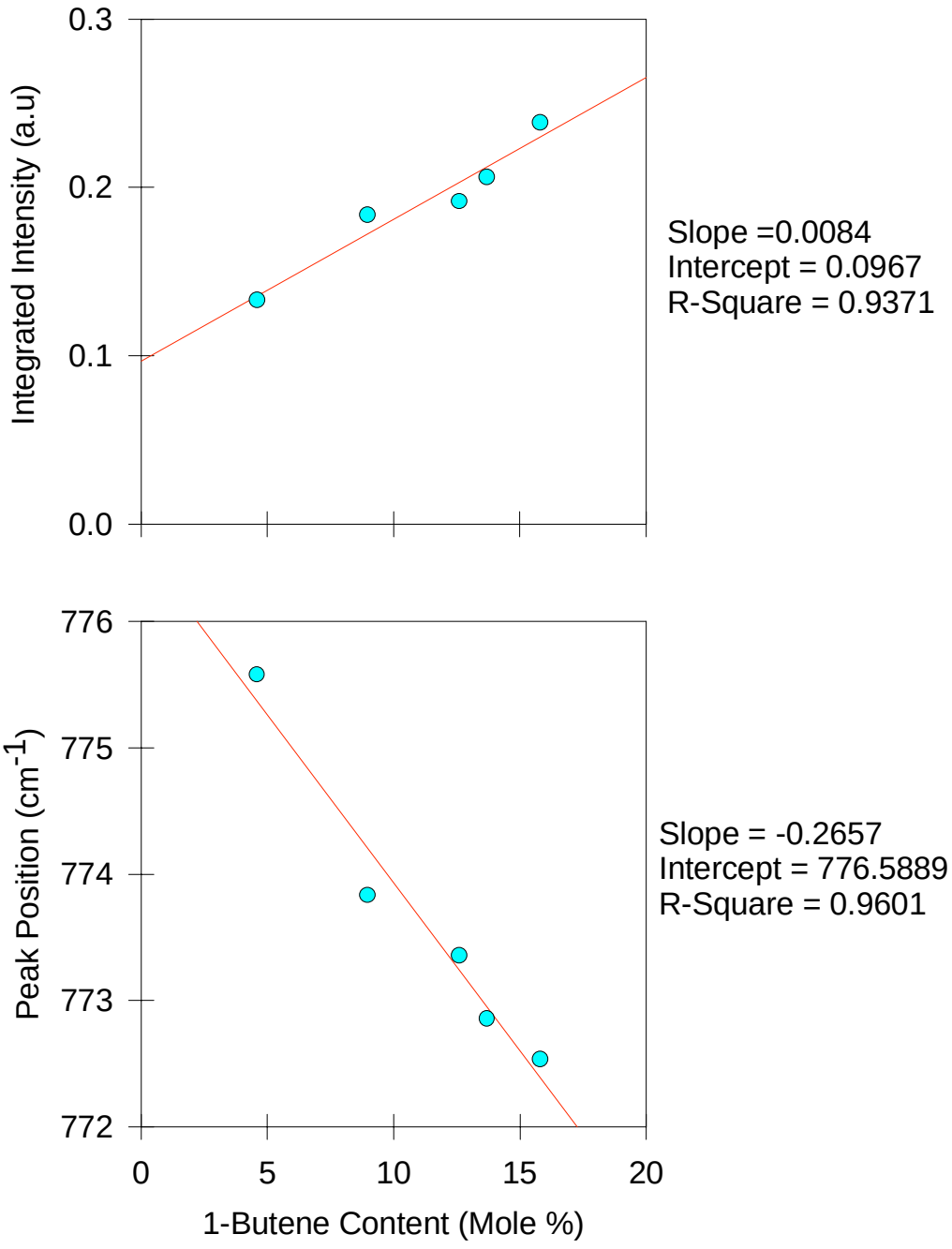

Figure 2 Peak position and integrated intensity of the 775cm^{-1} band as a function of comonomer content for the ethylene/1-butene copolymers

Next, several types of peaks were employed to achieve the best match for the band centered at 720cm^{-1}. After several attempts, it was concluded that more than one peak was necessary to fit this portion of the spectrum. Then, the same matching process was attempted with the next higher number of peaks, i.e., with two peaks. An excellent fit was obtained when a combination of two curve forms - an Exponentially Modified Gaussian and a HVL Chromatographic curve (HVL) - was employed. The HVL peak is mathematically represented as follows:

$$y = \frac{a_0 a_2 \exp\left[-0.5\left(\frac{x-a_1}{a_2}\right)^2\right]}{\sqrt{2\pi}\, a_1 a_3 \left[\frac{1}{\exp\left(\frac{a_1 a_3}{a_2^2}\right)-1} + 0.5\left[1+erf\left(\frac{x-a_1}{\sqrt{2}a_2}\right)\right]\right]} \qquad (2)$$

where the parameters a_0, a_1, a_2, and a_3 are given by the same definitions as for the EMG curve of Equation (1).

Thus, the melt spectrum was modeled as a combination of the above three types of curves. The best fits of the experimental melt spectra at different melt temperatures were obtained by appropriate variations in the parameters of the three curves. The values of the twelve parameters (from the three curves) from the first fit were plotted as a function of temperature to examine any possible trends in their behavior. It was found that most of the parameters (nine out of twelve) exhibited negligible variation with temperature and could be represented at all temperatures by an average value. The remaining three parameters were calculated as a function of temperature after fixing the values of the other nine parameters at the average values obtained in the first step. The three parameters were found to exhibit a linear dependence on temperature and their values at all test temperatures (25 to 160°C) were estimated from those linear equations. The fitted melt was constructed by combining the three curves obtained as described above.

In order to verify the quality of the procedure adopted, the fitted melt curves at several melt temperatures were compared to the experimentally obtained spectra at those temperatures. One example is given in Figure 3 for EB-883 with ~ 13 mole % 1-butene at 135°C. Excellent agreement is observed between data and calculations.

7.2.2 Determination of Amorphous Content

The fitted melt curves at all test temperatures were constructed following the above procedure. However, at a lower temperature, say 25°C, the sample is known to be semicrystalline. Therefore, in order to accurately represent the amorphous content at 25°C, the fitted melt must be multiplied by a factor that is proportional to the degree of crystallinity, χ_c at that temperature. An approximate value of χ_c at any temperature was obtained from the results of the thermal analysis experiments. Starting from that value, a trial and error process was adopted to determine the numerical factor that resulted in the best match at both ends of the fitted amorphous band with the experimental spectrum at that temperature. The fitted melt band multiplied by this factor yielded the amorphous band of the sample spectrum at that temperature. The amorphous band thus estimated is plotted along with the experimental spectrum at 30°C for EB-912 (~5 mole % 1-butene) in Figure 4(a).

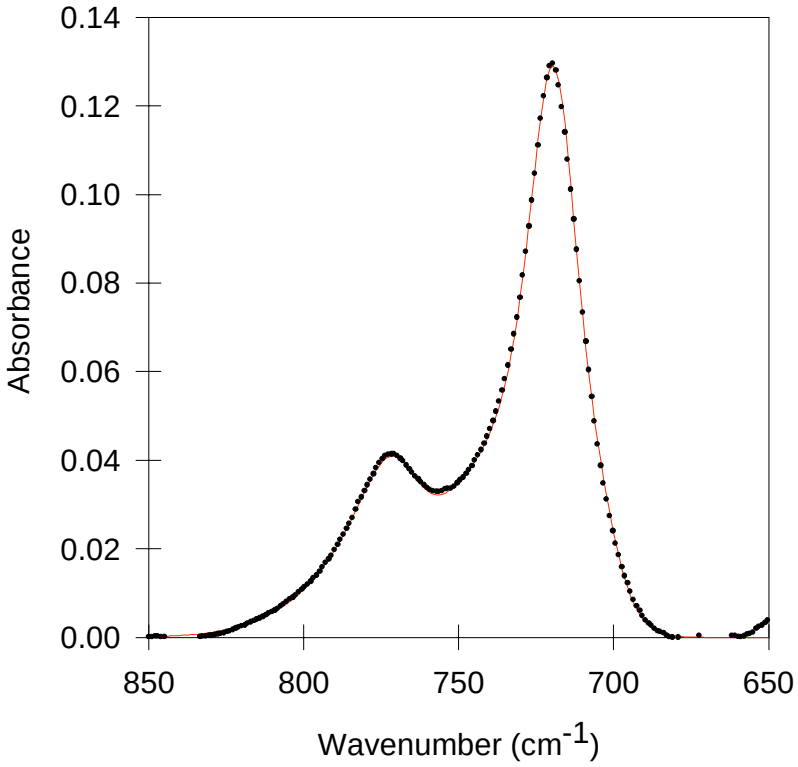

Figure 3 Comparison of fitted melt with the experimentally obtained melt spectrum at 135°C for EB-883 with ~ 13 mole % 1-butene (• Experimental; — Fitted)

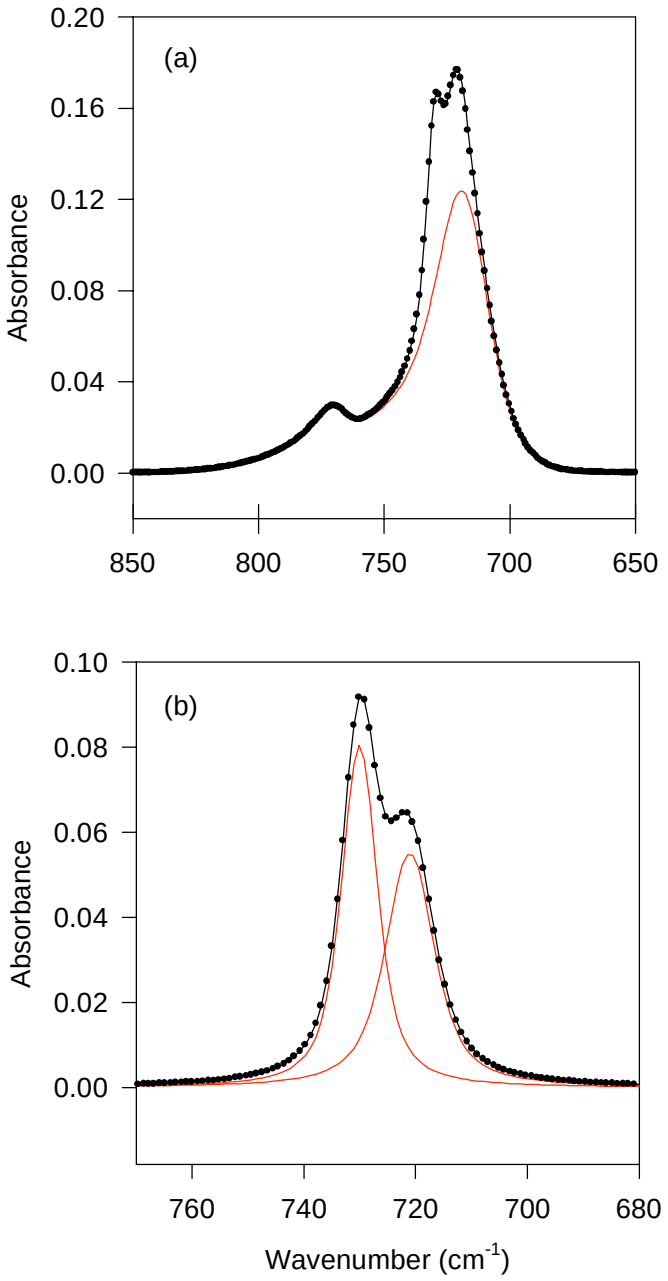

Figure 4 (a) The amorphous band estimated from mathematical modeling in comparison to the experimental semicrystalline spectrum (• Experimental spectrum; — Amorphous band from modeling), (b) the crystalline band after amorphous band subtraction with the fitted Voigt peaks (• Experimental Crystalline Band; — Fitted Voigt peaks) for EB-912 (~ 5 mole % 1-butene) at 30°C

7.3 The Crystalline Spectrum

The amorphous band at a given temperature obtained from above was subtracted from the semicrystalline sample spectrum at that temperature. The remainder of the spectrum after subtraction represents the chain vibrations in the crystalline fraction of the material and is comprised of a doublet of bands centered at 720 and 730 cm^{-1} as depicted in Figure 4(b). These bands were modeled using two Voigt functions, in a manner similar to that of the melt spectra. The details of the modeling are presented in a following section.

7.3.1 Degree of Crystallinity

The degrees of crystallinity, χ_c, of the copolymers were estimated from the areas of the amorphous and crystalline bands described so far. The following relationship due to Hagemann *et al.*[6] was employed for the crystallinity determination.

(3) $$\chi_c = \left(\frac{I_c}{I_c + \alpha\, I_a} \right)$$

where I_c, I_a = the crystalline and amorphous intensities respectively, and

α = a coefficient whose numerical value equals 1.2

The coefficient, α, that appears in Equation (3) was included to account for the fact that the intrinsic intensities of the crystalline and amorphous bands in the rocking region of the infrared spectra are not exactly identical to each other. Hagemann *et al.*[6] have estimated the numerical value for this coefficient using the relationship,

(4) $$\alpha = \frac{I_{722}^{\text{int}\,r} + I_{730}^{\text{int}\,r}}{I_{723}^{\text{int}\,r}}$$

where the I^{intr} stands for the intrinsic intensities of the bands at the corresponding wavenumbers. The crystallinities determined using Equation (3) for the ethylene/1-butene copolymers of varying branch contents - EB-912, EB-894 and EB-883 - during the first heating (quenched sample), slow cooling and second heating (slowly cooled sample) cycles are plotted as a function of temperature in Figure 5. These values for the three samples are also listed in Table 1, Table **2** and Table **3** respectively.

The crystallinities estimated from the three sets of experiments are found to be identical to each other, i.e., the crystallinity developed during quenching the sample is found to be the same as that developed on slowly cooling the sample from its melt. Furthermore, no hysteresis is observed between the crystallinities derived from the heating and cooling cycles. However, it may be recalled that the crystallinities estimated from similar experiments using thermal analysis studies (discussed in Chapter 5) clearly indicate the hysteresis as well as the influence of the cooling rate on the crystallinities of the copolymers. This discrepancy between the results from the two techniques may be understood based on the higher uncertainty associated with the infrared crystallinities, with both experimental parameters as well as the multiple deconvolution processes contributing to it.

7.3.2 Degree of Crystallinity - Effect of Comonomer Content

A comparison of the χ_c values listed in Table 1 through Table 3 clearly reveals the influence of comonomer concentration on the level of crystallinity in the copolymers. A marked decrease in crystallinity occurs as the comonomer content in the copolymer is increased as shown in Figure 6(a). Furthermore, a comparison of the infrared spectra of the copolymers at 25°C (Figure 6(b)) clearly indicates that the intensity of the band at 730 cm^{-1} associated with the orthorhombic crystals diminishes with increasing branch content. It is reassuring to note that the integrated intensity of the band at 775cm^{-1} due to the ethyl branch vibrations systematically increases with increasing branch concentration (also shown in Figure 2).

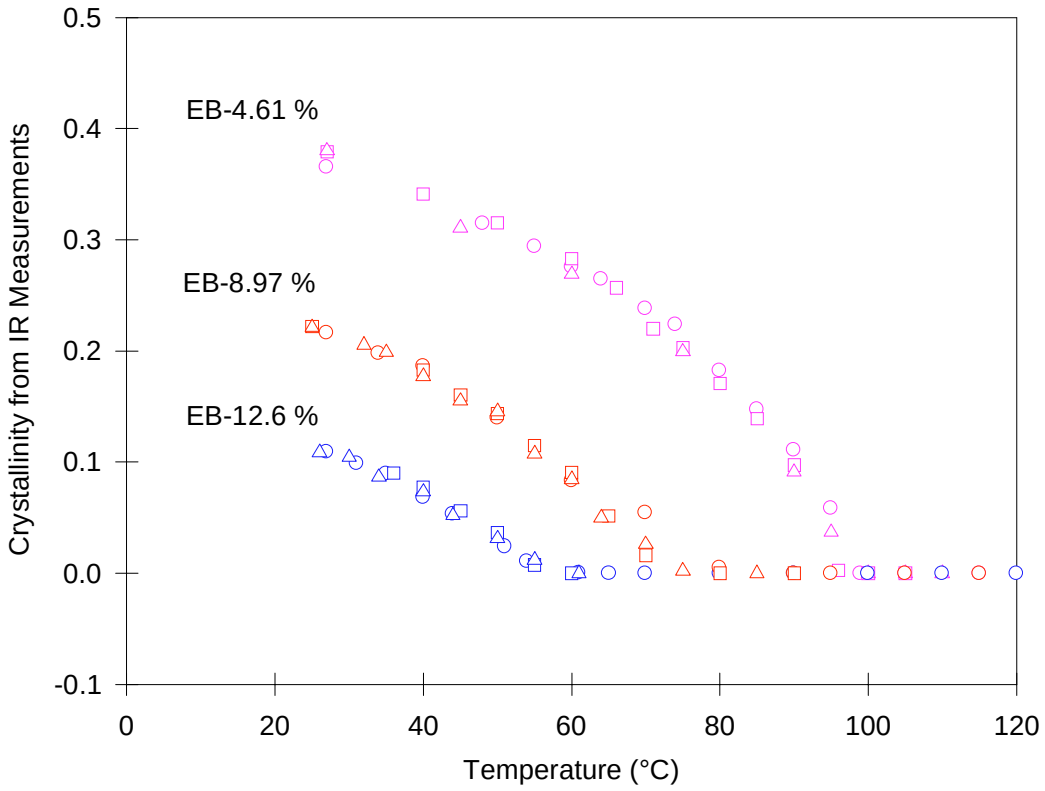

Figure 5 Crystallinity as a function of temperature for the ethylene/1-butene copolymers (o First heating; Cooling; Δ Second heating cycles)

Table 1 Crystallinities for EB-912 (with ~ 5 mole % 1-butene) during (a) Heating of a quenched sample (b) Slow Cooling (c) Heating of a slowly cooled sample (A rate of 1.5°C/min was used for all three processes)

First Heating		Cooling		Second Heating	
T (°C)	χ_c	T (°C)	χ_c	T (°C)	χ_c
27	0.37	27	0.38	27	0.38
48	0.31	40	0.34	45	0.31
55	0.29	50	0.32	60	0.27
60	0.28	60	0.28	75	0.20
64	0.26	66	0.26	90	0.09
70	0.24	71	0.22	95	0.04
74	0.22	75	0.20	100	0.00
80	0.18	80	0.17	105	0.00
85	0.15	85	0.14	110	0.00
90	0.11	90	0.10	115	0.00
95	0.06	96	0.00	124	0.00
99	0.00	100	0.00	135	0.00
105-160	0.00	105-160	0.00	144-160	0.00

Table 2 Crystallinities for EB-894 (with ~ 9 mole % 1-butene) during (a) Heating of a quenched sample (b) Slow Cooling (c) Heating of a slowly cooled sample (A rate of 1.5°C/min was used for all three processes)

First Heating		Cooling		Second Heating	
T (°C)	χ_c	T (°C)	χ_c	T (°C)	χ_c
27	0.22	25	0.22	25	0.22
34	0.20	40	0.18	32	0.21
40	0.19	45	0.16	35	0.20
45	0.16	50	0.14	40	0.18
50	0.14	55	0.11	45	0.16
55	0.11	60	0.09	50	0.15
60	0.08	65	0.05	55	0.11
65	0.06	70	0.02	60	0.08
70	0.05	80	0.00	64	0.05
75	0.01	90	0.00	70	0.03
80	0.01	100	0.00	75	0.00
90	0.00	110	0.00	80	0.00
95-160	0.00	120-160	0.00	85-160	0.00

Table 3 Crystallinities for EB-883 (with ~ 13 mole % 1-butene) during (a) Heating of a quenched sample (b) Slow Cooling (c) Heating of a slowly cooled sample (A rate of 1.5°C/min was used for all three processes)

First Heating		Cooling		Second Heating	
T (°C)	χ_c	T (°C)	χ_c	T (°C)	χ_c
27	0.11	36	0.09	26	0.11
31	0.10	40	0.07	30	0.10
35	0.09	45	0.05	34	0.08
40	0.07	50	0.03	40	0.06
44	0.06	55	0.01	44	0.05
51	0.04	60	0.00	50	0.02
54	0.03	65	0.00	55	0.01
61	0.00	70	0.00	61	0.00
65	0.00	80	0.00	64	0.00
70	0.00	90	0.00	69	0.00
80-160	0.00	100-160	0.00	74-160	0.00

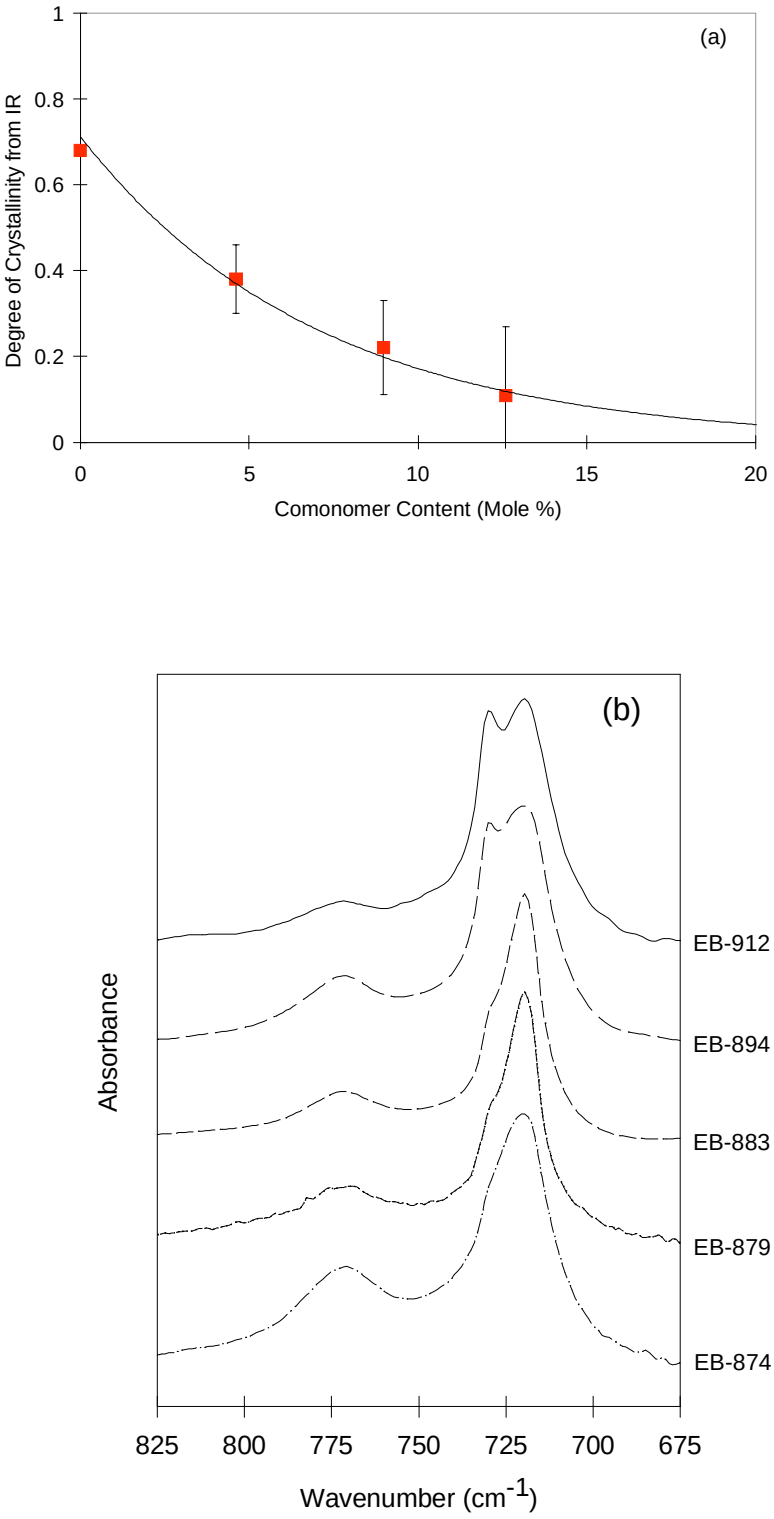

Figure 6 (a) Infrared crystallinities of the ethylene/1-butene copolymers as a function of comonomer content, (b) infrared spectra at 25°C for the ethylene/1-butene copolymers with varying branch contents

7.3.3 Modeling the Orthorhombic Doublet

It was mentioned earlier that the crystalline doublet remaining after the subtraction of the amorphous band from the semicrystalline sample spectrum was modeled using two Voigt peaks. The mathematical representation of a Voigt function is given below.

$$y = \frac{\int_{-\infty}^{\infty} \frac{a_0 \exp(-y^2)dy}{a_3^2 + \left[\left(\frac{x - a_1}{a_2}\right) - y\right]^2}}{\int_{-\infty}^{\infty} \frac{\exp(-y^2)dy}{a_3^2 + y^2}} \qquad (5)$$

where the parameters, a_0, a_1, a_2 and a_3 represent the same quantities as in Equations (1) and (2). The bandwidths and distortions of the two Voigt peaks used were kept constant at all temperatures to minimize the subjectivity of the curve-fitting procedure. Variations in crystallinity as a function of temperature were accounted for by varying the peak areas (heights) of the Voigt peaks.

Thus, the semicrystalline sample spectrum at any temperature was modeled using a combination of five curves - three for the amorphous fraction (two EMGs and one HVL curves) and two for the crystalline fraction (two Voigt peaks). The same procedure was adopted for analyzing the sample spectra collected during the cooling and second heating cycles.

7.4 Problems in Highly Branched Copolymers

Some difficulties were encountered when the comonomer concentration of the copolymer exceeded ~ 9 mole percent. The infrared spectra of these samples were much broader compared to the other three copolymers discussed above. As a result, it was inappropriate to use the same curve fitting parameters used for those latter copolymers.

Similar results have been reported by Howard and Crist[1] in the Wide Angle X-Ray Diffraction (WAXD) spectra of such copolymers. These authors have recognized that the lower levels of crystallinity and the broader diffraction peaks in the WAXD spectra of highly branched copolymers hamper quantitative measurements of any kind. As a result, they even chose to orient the samples prior to the diffraction experiments to enhance the extent of crystallinity and the relative sharpness of the diffraction peaks. It has been established in the present study (from the thermal analysis described in Chapter 5) that the copolymers with > 9 mole % butene are characterized by extremely low levels of crystallinity ($\chi_c \leq 0.09$ at 20°C). Furthermore, the Atomic Force Micrographs (from Chapter 6) of these materials were found to be predominated by crystals whose lateral dimensions as well as thicknesses were reduced to such an extent that they were barely visible in the micrographs. A parallel study of the crystal structure of these copolymers by means of WAXD experiments also indicates that the packing density within the crystals diminishes considerably as the branch content of the copolymers is increased.[5,7] It is possible that the dilation of the unit cell parameters (decrease in the crystal density) with increasing branch content results in the increased amplitudes of vibration of the ethylene sequences in the unit cell thereby causing a broadening of the spectrum[1,2] and even a slight shifting of some of the bands.

7.5 Second Crystal Structure

The crystalline bands (after subtraction of the amorphous band) discussed in Section 7.3.1 were analyzed further to determine the presence (or absence) of crystals with a second unit cell structure, in addition to the usual orthorhombic form. Our approach was based on the examination of the ratios of the integrated intensities of the doublet bands at 730 and 720 cm^{-1}. This ratio, I_{730}/I_{720}, for the copolymers were compared[5] to those of linear polyethylene (LPE) and an *n*-paraffin, octacosane, both of which are known to exhibit an orthorhombic crystal structure[8,9,10] at room temperature.

The infrared spectra of these two materials were obtained at several temperatures ranging from 25 to 160°C and are depicted in Figure 7 for the *n*-paraffin. The hexagonal

rotator phase that acts as an intermediate in the melting of the *n*-paraffin is clearly observed at ~ 719 cm^{-1}. This band is distinctly different from both the orthorhombic doublet as well as from the broad amorphous band of the melt.

The amorphous bands (for LPE only) were estimated and subtracted from the spectra using the procedure described in Section 7.1. The remainder of the spectrum, comprised of a doublet of peaks centered at 730 and 720 cm^{-1} represents the chain vibrations in the crystalline regions of the materials. The ratios, I_{730}/I_{720}, were estimated and are found to vary closely around a value of one (until the melt) for both materials, as shown in Figure 8. This value implies that the band splitting in the case of octacosane and LPE results in two equivalent bands, represented by the doublet at 730 and 720 cm^{-1}.

I_{730}/I_{720} was also estimated for all the copolymers in the entire temperature range, for all three sets of experiments (first heating, cooling and second heating cycles). These values are plotted as a function of temperature for the three ethylene/1-butene copolymers in Figure 9 through Figure 11, and also tabulated in Table 4 through Table 6. The ratios, I_{730}/I_{720} calculated for the copolymers (Table 4 through Table 6) are clearly less than one at all temperatures, implying that the integrated intensity of the peak at 720cm^{-1} is larger than that of the peak at 730cm^{-1}. The latter peak is known to be entirely due to vibrations of the ethylene sequences associated with the orthorhombic crystal structure. In the absence of any other crystal form in the sample, the ratio must equal one as in the case of octacosane and LPE discussed in the previous paragraph. Therefore, it can be concluded that a second crystal structure co-exists with the orthorhombic crystal form in the copolymers. The second crystal form contributes to the integrated intensity of the band at 720 cm^{-1} to an extent determined by the comonomer content of the sample.

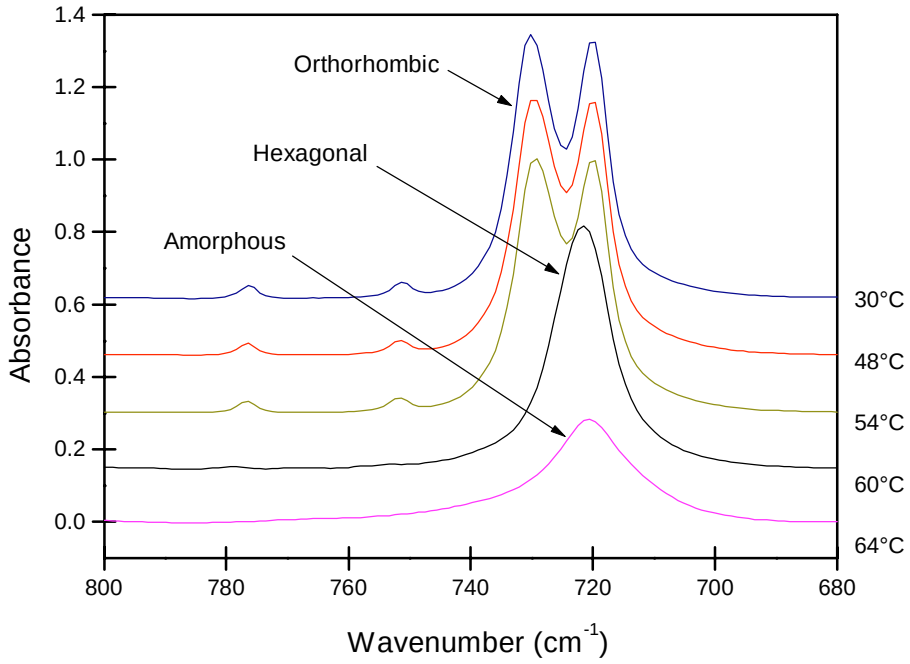

Figure 7 Infrared spectra of octacosane at various temperatures (as indicated) (From Dr. A. Alizadeh)

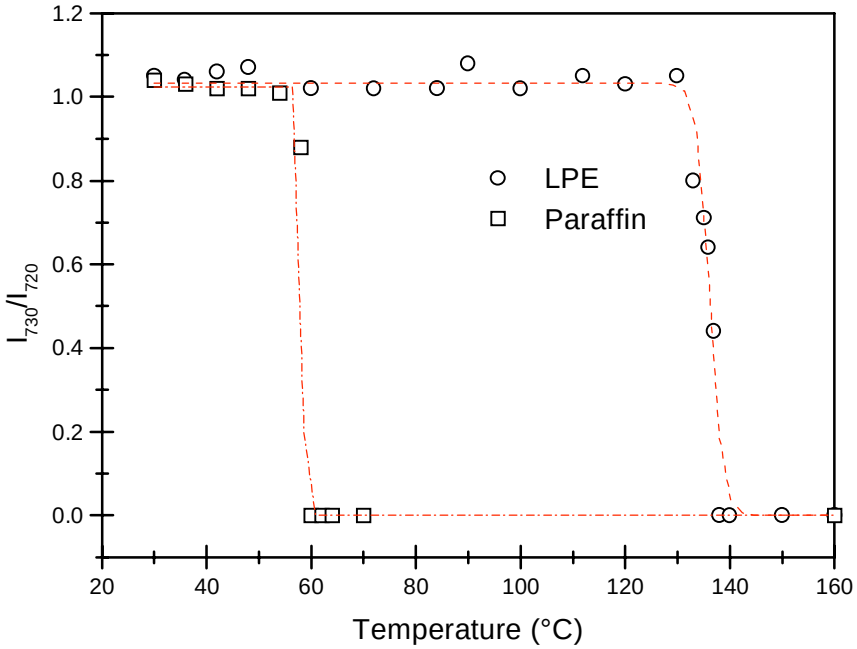

Figure 8 Ratios of I_{730}/I_{720} for linear polyethylene and an *n*-paraffin, octacosane, at various temperatures (from Dr. A. Alizadeh)

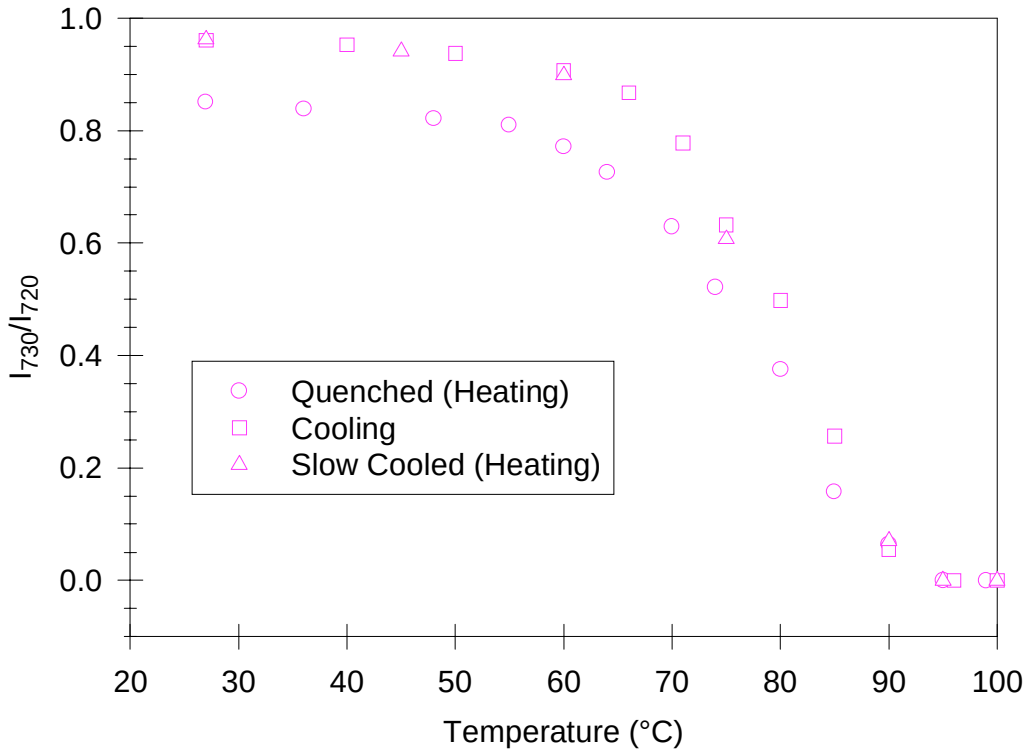

Figure 9 Ratio of I_{730}/I_{720} for EB-912 (with ~ 5 mole % 1-butene) during (o) Heating of a quenched sample ( ) Slow Cooling (Δ) Heating of a slowly cooled sample (A rate of 1.5°C/min was used for all three processes)

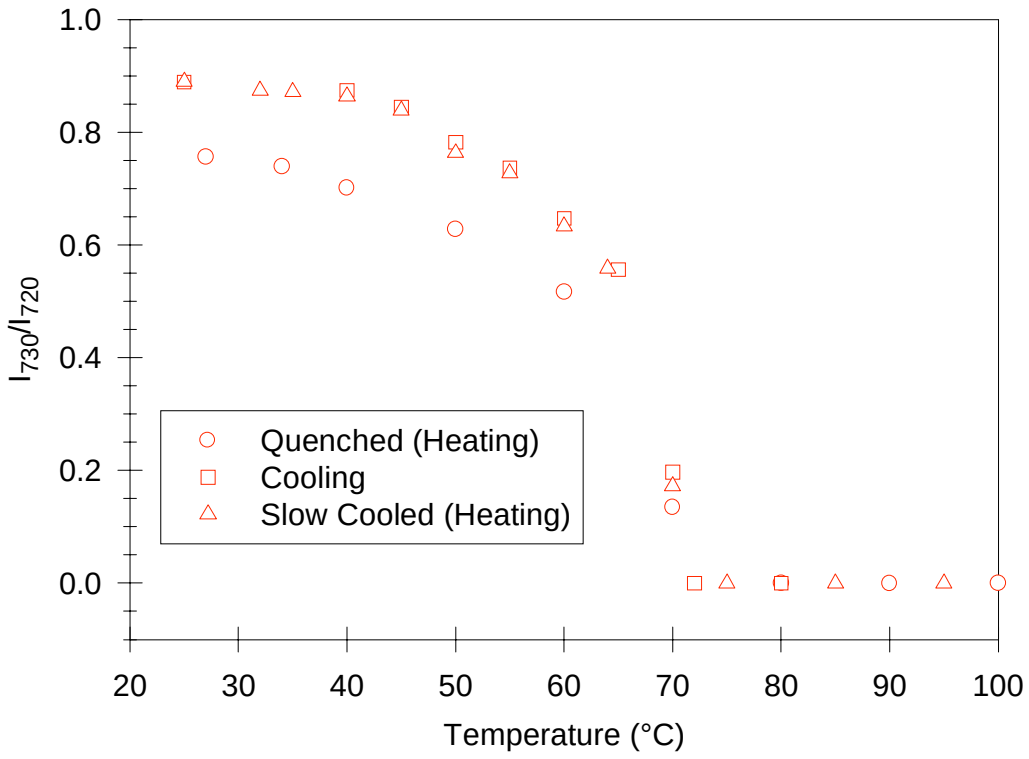

Figure 10 Ratio of I_{730}/I_{720} for EB-894 (with ~ 9 mole % 1-butene) during (o) Heating of a quenched sample ( ) Slow Cooling (Δ) Heating of a slowly cooled sample (A rate of 1.5°C/min was used for all three processes)

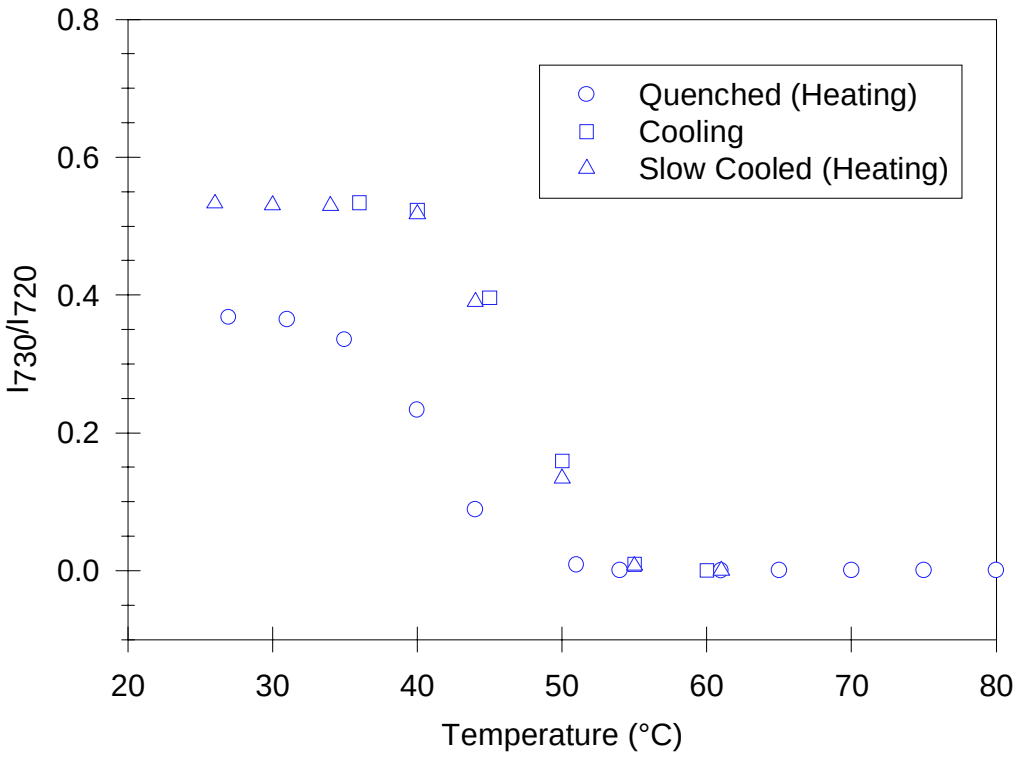

Figure 11 Ratio of I_{730}/I_{720} for EB-883 (with ~ 13 mole % 1-butene) during (o) Heating of a quenched sample ( ) Slow Cooling (Δ) Heating of a slowly cooled sample (A rate of 1.5°C/min was used for all three processes)

Table 4 Ratios of the integrated intensity of the crystalline bands at 730 and 720 cm^{-1} in the infrared spectrum of EB-912 (~ 5 mole % 1-butene)

First Heating		Cooling		Second Heating	
T(°C)	I_{730} / I_{720}	T(°C)	I_{730} / I_{720}	T(°C)	I_{730} / I_{720}
27	0.851	27	0.961	27	0.962
36	0.839	40	0.953	45	0.942
48	0.822	50	0.937	60	0.899
55	0.810	60	0.908	75	0.607
60	0.771	66	0.867	90	0.071
64	0.726	71	0.778	95	0.000
70	0.629	75	0.632	100	0.000
74	0.521	80	0.498	105	0.000
80	0.375	85	0.256	110	0.000
85	0.158	90	0.055	115	0.000
90	0.064	96	0.000	120	0.000
95	0.000	100	0.000	125	0.000
99-160	0.000	105-160	0.000	130-160	0.000

Table 5 Ratios of the integrated intensity of the crystalline bands at 730 and 720 cm^{-1} in the infrared spectrum of EB-894 (~ 9 mole % 1-butene)

First Heating		Cooling		Second Heating	
T(°C)	I_{730} / I_{720}	T(°C)	I_{730} / I_{720}	T(°C)	I_{730} / I_{720}
27	0.754	25	0.889	25	0.890
34	0.747	40	0.874	32	0.874
40	0.731	45	0.844	35	0.871
50	0.628	50	0.782	40	0.864
60	0.516	55	0.736	45	0.839
70	0.135	60	0.647	50	0.763
80	0.000	65	0.556	55	0.728
90	0.000	70	0.197	60	0.633
100	0.000	72	0.000	64	0.558
110	0.000	80	0.000	70	0.172
120	0.000	85	0.000	75	0.000
130-160	0.000	90-160	0.000	80-160	0.000

Table 6 Ratios of the integrated intensity of the crystalline bands at 730 and 720 cm^{-1} in the infrared spectrum of EB-883 (~ 13 mole % 1-butene)

First Heating		Cooling		Second Heating	
T(°C)	I_{730} / I_{720}	T(°C)	I_{730} / I_{720}	T(°C)	I_{730} / I_{720}
27	0.368	36	0.534	26	0.533
31	0.365	40	0.523	30	0.531
35	0.335	45	0.396	34	0.529
40	0.233	50	0.159	40	0.518
44	0.088	55	0.009	44	0.390
51	0.009	60	0.000	50	0.134
54	0.000	65	0.000	55	0.007
61	0.000	70	0.000	61	0.000
65-160	0.000	75-160	0.000	64-160	0.000

7.6 Determination of the Second Crystal Structure

The results presented so far clearly indicate the presence of a second crystal structure (in addition to the usual orthorhombic one) in the copolymers examined. The relative proportion of this second type of crystals present in a sample at any temperature was quantitatively determined in the present study by adopting the following procedure.

The first step involves a deconvolution of the crystalline doublet (comprising the bands at 730 and 720 cm^{-1}) using a curve-fitting procedure. This method is based on the results from the previous section that clearly indicated significant contributions (the extent of contribution depends on the comonomer content of the sample) from the second crystal structure to the total integrated intensity of the crystalline bands. Furthermore, since the band at 730 cm^{-1} is known to be entirely due to chain vibrations of the orthorhombic crystals, the contribution of the second crystal form must be present as an overlapping band with the one at 720 cm^{-1}. The aim of the deconvolution process is to determine the exact contribution of this crystal structure to the integrated intensity of the crystalline doublet, more specifically, to the band at 720 cm^{-1}. For this purpose, two peaks identical to the Voigt peak at 730 cm^{-1} (one of them shifted to 720cm^{-1}) were used. All the curve-fitting parameters for these two peaks were locked. In addition a third Voigt peak was also employed to represent the intensity contribution from the second crystal fraction. The best fit obtained for the third (Voigt) peak from the deconvolution process is a direct representation of the integrated intensity of the chain vibrations associated with the second crystal structure. This peak was found to be centered at ~ 719-721 cm^{-1} for the copolymers studied. An example of such a deconvolution is shown in Figure 12 for the infrared spectrum of EB-883 at 25°C.

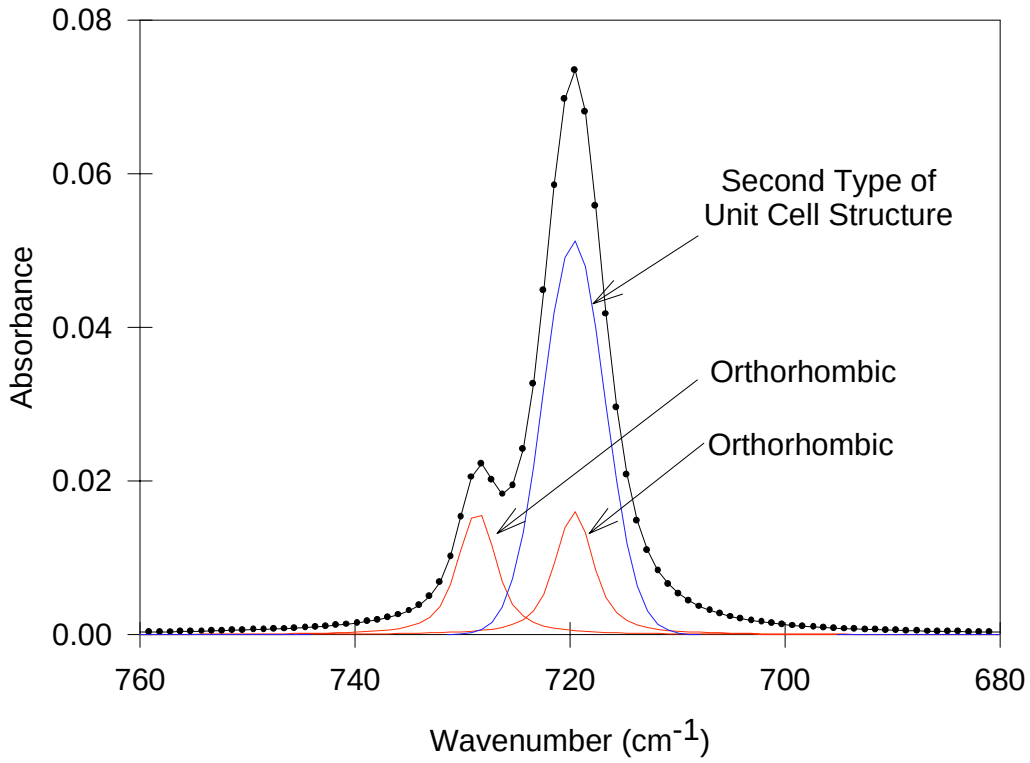

Figure 12 Deconvolution of the crystalline portion of the infrared spectrum. The sample indicated is EB-883 (~ 9 mole % 1-butene) at 25°C

In addition, it is now clearly evident that the band at 730 cm^{-1} is associated entirely with the fraction of orthorhombic crystals present in the material, and that the second crystal structure contributes to the integrated intensity of the crystalline band at 720 cm^{-1}. Then, the band at 720 cm^{-1} may be viewed as being comprised of contributions from crystals with the orthorhombic and the second type of unit cell structures. Therefore, the ratio, I_{730}/I_{720} may be written as follows:

$$R = \frac{I_{730}}{I_{720}} = \frac{I_{orthorhombic}}{I_{orthorhombic} + I_{second\ crystal\ structure}}$$

Substituting the integrated intensity of the 730 cm^{-1} band from the infrared spectrum of the sample, in the above expression yields the integrated intensity of the second crystal form as shown below,

$$I_{second\ crystal\ structure} = I_{orthorhombic}\left(\frac{1-R}{R}\right)$$

Then, the ratio, ($I_{\text{second crystal structure}}/I_C$) represents the relative contribution of the second crystal structure to the total crystalline fraction in the material. These ratios estimated for the quenched samples, i.e., during the first heating cycle, are plotted as a function of temperature in Figure 13 for the ethylene/1-butene copolymers and are also listed in Table 7. It is found that the integrated intensity of the band associated with the second crystal structure increases with branch content and with temperature, while that of the orthorhombic crystal structure decreases simultaneously.

Furthermore, it is noted that the integrated intensity of the Voigt peak representing the second crystal structure determined from the deconvolution process (described in the first part of this section) was found to be in close agreement with ($I_{\text{second crystal structure}}$) determined from the above calculation.

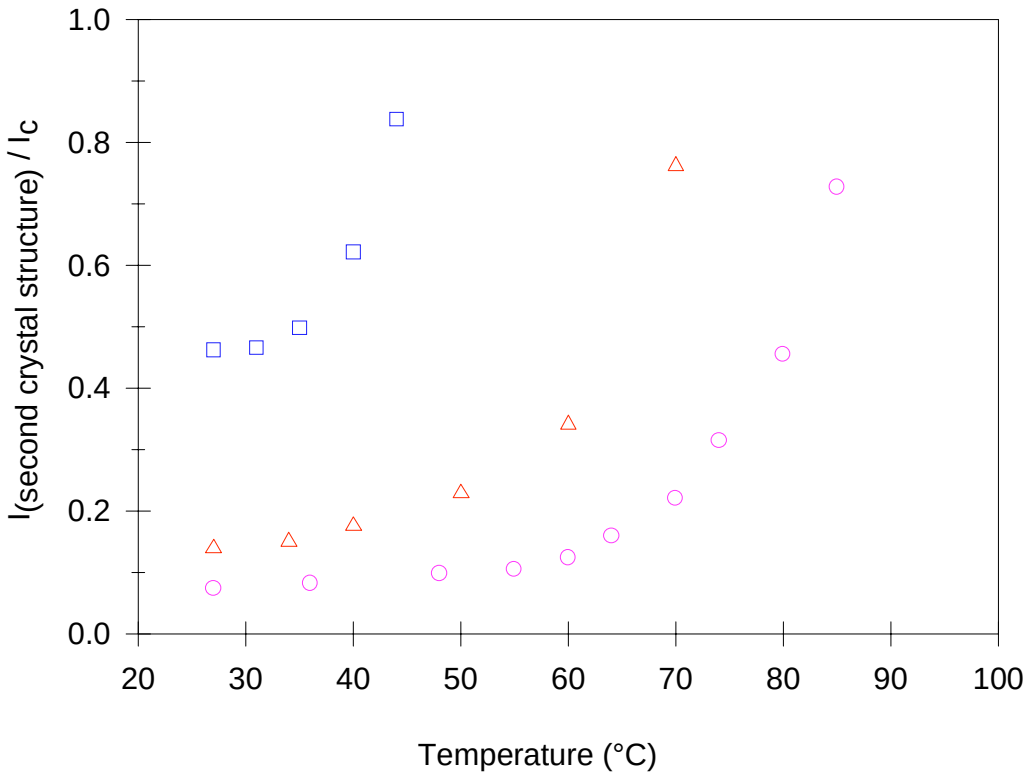

Figure 13 Variation of the integrated intensity of the second crystal structure as a function of temperature for the copolymers, (o) EB-912 (~ 5 mole % 1-butene), (Δ) EB-894 (~ 9 mole % 1-butene) and ( )EB-883 (~ 13 mole % 1-butene)

Table 7 Relative contribution of the second crystal structure to the total crystalline fraction for the quenched ethylene/1-butene copolymers

EB-883		EB-894		EB-912	
T(°C)	I_{other} / I_{720}	T(°C)	I_{other} / I_{720}	T(°C)	I_{other} / I_{720}
27	0.632	27	0.244	27	0.137
31	0.635	34	0.261	36	0.150
35	0.665	40	0.299	48	0.178
40	0.767	50	0.372	55	0.190
44	0.912	60	0.517	60	0.220
51	-	70	0.865	64	0.275
54	-	75	-	70	0.359
61	-	80	-	74	0.479
65	-	85	-	80	0.625
70	-	90	-	85	0.842
75-160	-	96-160	-	90-160	-

7.7 Discussion

7.7.1 Dual Crystal Structure

The different types of crystal morphologies and the early models describing the chain folding process in polymers were extensively discussed in Chapter 2. It is now well established that homopolymers crystallized from the melt under quiescent conditions predominantly adopt the chain-folded lamellar structure.[11,12,13] However, the presence of defects such as comonomers (in the present case) along the polymer backbone and/or very high molecular weights hinders the regular chain folding process and yields thinner lamellae with decreased lateral dimensions,[14,15] or in the limiting cases, alternate crystal morphologies such as the bundled-type crystals discussed in Chapter 5. The decreased thickness of such crystals has been widely associated with an observable expansion of the unit cell lattice parameters (more specifically *a* and *b*) obtained from Wide Angle X-Ray Diffraction measurements.[1,16,17] Such a correlation was originally proposed by Bunn[18] in the early 1950's, and has since then been verified and extended by other investigators. A variety of explanations for the expansion of the lattice parameters have been proposed, including surface stresses.[18,19,20,21,22] Some authors[23,24,25,26] have even interpreted the *a*-axis expansion and the accompanying decrease in crystallite thickness as an indication that the branches are incorporated into the crystal lattice. Such a conclusion, however, is not a definite and necessary consequence of the above observations. The decrease in crystal thickness could be a direct result of shorter lengths of the available crystallizable sequences. The expansion of the *a*-axis could be a result of the increased strain resulting from the aggregation of the co-units at the interface of the thin crystals.[27] Furthermore, the lattice expansion with crystallization temperature has been reported even in the case of linear polyethylene (LPE),[19] where there is no branch species. In this case, the expansion is explained on the basis of fold-fold steric repulsions.

It is clear from the above discussion that the crystals formed during the secondary crystallization of the copolymers studied are highly strained, thinner and less perfect compared to the chain-folded lamellar crystals formed during the primary crystallization. These relatively less perfect crystals are very likely to adopt a crystal structure other than

the orthorhombic form usually associated with linear polyethylene. Keeping in mind the high degree of constraint associated with the crystals, it is possible that these crystals may be characterized by either the monoclinic or hexagonal unit cell structures, both of which have been reported to be present in polyethylene crystallized under conditions of (macroscopic) stress. The monoclinic modification of linear polyethylene (LPE), which is characterized by a band at 715cm^{-1} in the infrared spectrum, was originally proposed by Teare and Holmes[28] and by Turner Jones[29] four decades ago and has since then been the subject of several investigations. The influence of various parameters such as molecular weight[30], crystallization conditions[30,31,32,33] (cooling rate, crystallization temperature, annealing time etc.) and branch content[16,17] (in a copolymer) on the relative proportion of monoclinic type crystals in a given sample have been extensively studied. It is suggested from the results of these investigations that increasing the molecular weight, cooling rate and/or branch concentration of the samples favors the generation of the monoclinic modification.

The hexagonal unit cell structure, which was mentioned above as the other possible unit cell modification for such crystals, is also found in samples crystallized under conditions of stress.[34,35] This modification suffers from the occurrence of a large number of conformational defects and from the lack of long range order. It has been suggested by several investigators[36,37,38,39] that this crystal structure acts as an intermediate phase in the crystallization of LPE (under stress) from the melt to an extended chain crystal. Similar observations have been made on the crystal transitions involving the hexagonal rotator phase in *n*-alkanes.[40,41,42] Some authors have indicated[39] that the orthorhombic-to-hexagonal transition occurring close to the melt temperatures in LPE (under stress) is similar to the transitions involving the hexagonal rotator phase in *n*-alkanes.

The second crystal structure present in the copolymers used in the current study is compatible with a hexagonal type unit cell based on the following comparison. The (third) Voigt peak resulting from the deconvolution process (Figure 12) described in Section 7.6 is compared to that of the hexagonal rotator phase in the *n*-paraffin, octacosane[5] (Figure 7). It may be recalled that this Voigt peak at 719 - 721 cm^{-1} is a direct representation of the integrated intensity due to chain vibrations in the second

crystal structure present in the copolymer. The rotator phase that acts as an intermediate in the melting of the *n*-paraffin is clearly observed at ~ 719 cm^{-1} in Figure 7. Comparing the respective bands from the two figures, it is found that the shapes and positions of the two peaks are identical to each other, within experimental error. Therefore, these results suggest that the second crystal structure co-existing with the orthorhombic form in the copolymers is most likely to be characterized by the hexagonal unit cell type.

The relative contribution of the second crystal structure to the total crystalline fraction in the samples is depicted in Figure 13 for the ethylene/1-butene copolymers. The increase in the relative proportion of these crystals with increasing comonomer content is easily explained based on the ideas discussed in the previous paragraphs of this section. The regular chain folding process is hampered by the increasingly higher comonomer content, thereby resulting in the generation of a larger proportion of thinner and less perfect crystals. The large stresses associated with these crystals causes them to adopt a distorted orthorhombic or even an alternate crystal structure such as the hexagonal type as suggested by the results of the present study.

It is also noted from Figure 13 that the relative contribution of the second crystal structure increases with temperature, for a given copolymer. This observation is not as easily understood as the previous one. It cannot be explained based on the melting of the hexagonal type crystals, since it is contrary to our expectation that these crystals continue to exist at higher temperatures than the more regularly packed orthorhombic crystals (compare to Figure 9 through Figure 11 where the relative proportion of orthorhombic crystals decreases with temperature). It is possible that the ordered trans sequences of the orthorhombic crystals are transformed to a disordered trans conformation during heating. These disordered sequences may be present either in the hexagonal type or in the melt - this information is not obtained by means of the infrared technique. The above explanation is also comparable to the one proposed by Tashiro *et al*.[43] to explain the structural changes in polyethylene during isothermal crystallization. These authors have suggested that the crystallization of PE from the melt occurs first by the generation of conformationally disordered short trans sequences, which subsequently aggregate into the more regularly packed orthorhombic type crystals.

7.7.2 Effect of Cooling Rate

A comparison of the I_{730}/I_{720} values in Table 4 through Table 6 indicates that the proportion of orthorhombic crystals formed during quenching is considerably less than that generated in a slowly cooled sample. In other words, the second type of crystals (less perfect), associated with the hexagonal unit cell structure is present to a greater extent in the quenched material. This observation is consistent with the expectation that more disordered crystals are generated during quenching, as compared to slow cooling of the samples. Slower rates of cooling allow a sample to spend longer times at a higher temperature than that afforded for a quenched sample. As a result, the crystallization of a slowly cooled sample may be visualized as occurring at a higher temperature than that of a quenched one. According to Flory's theory of copolymer crystallization[44,45], the critical sequence length, ζ^*, that can be in equilibrium with the melt at high temperatures is longer than those at much lower temperatures. Those long sequences can form chain-folded crystals with the more ordered orthorhombic unit cell structure. However, for a rapidly cooled (quenched) sample, the crystallization may be imagined as occurring at a relatively lower temperature. The critical sequence lengths are accordingly much lower, resulting in the formation of thinner and less perfect crystals.

7.7.3 Effect of Comonomer Content

It is expected that an increase in the branch concentration of the copolymer should yield a higher proportion of less perfect crystals, which are associated with the second crystal form. This expectation is confirmed by the following observations from the present study. The values of $I_{\text{second crystal type}}/I_c$ depicted in Figure 13 clearly show that the relative fraction of the second type of crystals increases systematically with increasing comonomer content. Accordingly, the intensity of the peak at 730 cm^{-1} associated with the ordered orthorhombic crystal structure (in Figure 4(b)) is found to gradually decrease in intensity with increasing branch content. This is further supported

by the decreasing proportion of orthorhombic crystals represented by the ratio, I_{730}/I_{720} with increasing comonomer contents as shown in Figure 14.

The results from the FTIR study on the ethylene/1-butene copolymers were discussed in this chapter. The next chapter, which is the last one of this dissertation, presents the conclusions arrived at in the present study.

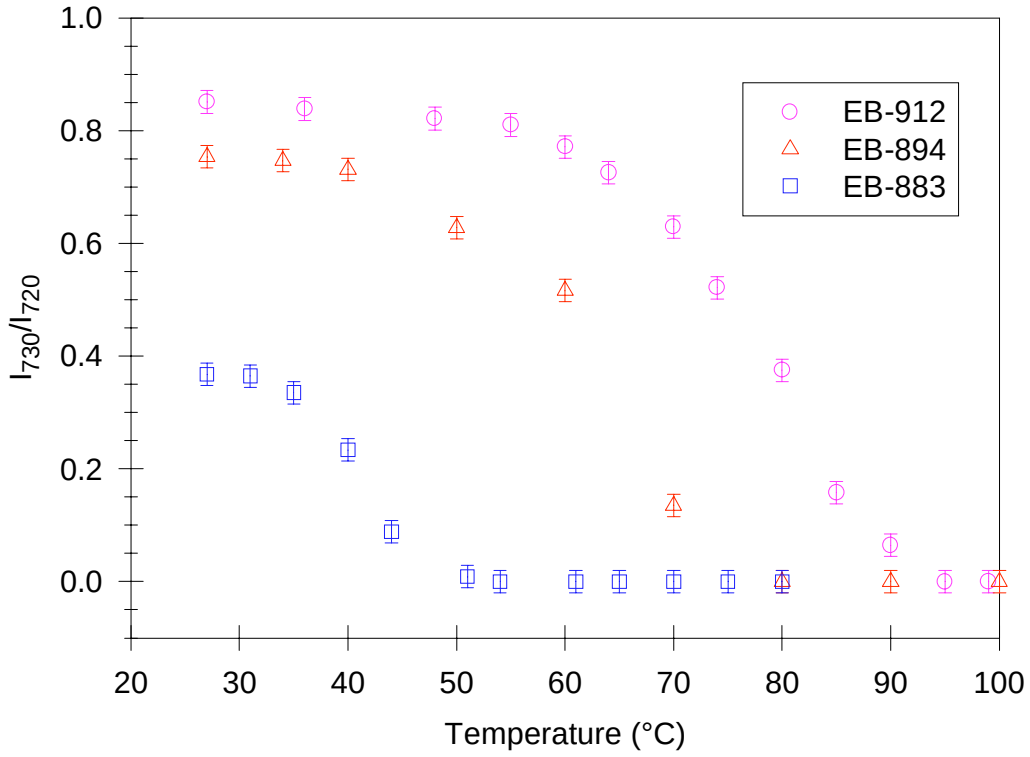

Figure 14 Variation in the ratio I_{730}/I_{720} with comonomer content for the ethylene/1-butene copolymers

[1] P. R. Howard and B. Crist, *J. Polym. Sci. Polym. Phys. Ed.*, **27**, 2269 (1989)
[2] J. L. Koenig, "*Spectroscopy of Polymers"*, American Chemical Society, Washington, DC. (1992)
.[3] R. G. Snyder, "*Methods of Experimental Physics*", Eds., L. Marton and C. Marton, Academic Press, New York, Vol. 16; Part A, Chapter 3 (1980)
[4] D. I. Bower and W. F. Maddams, "*The Vibrational Spectroscopy of Polymers*", Ed., R. W. Cahn, E. A. Davis and I. M. Ward, Cambridge University Press, Cambridge, 1989
[5] A. Alizadeh *et al.*, *Manuscript in Preparation*
[6] H. Hagemann, R. G. Snyder, A. J. Peacock and L. Mandelkern, *Macromolecules*, **22**, 3600 (1989)
[7] A. Alizadeh, J. Xu, L. Richardson, S. McCartney, H. Marand and S. Chum, *Submitted to Macromolecules*
[8] C. W. Bunn and T. C. Alcock, *T. Faraday Soc.*, **41**, 317 (1945)
[9] C. W. Bunn, *T. Faraday Soc.*, **35**, 482 (1939)
[10] A. Muller, *Proc. R. Soc. London*, **A120**, 137 (1928)
[11] A. Keller, *Phil. Mag.*, **2**, 1171 (1957)
[12] A. Keller, *Rep. Prog. Phys.*, **31**, 623 (1968)
[13] J. C. Wittmann and B. Lotz, *J. Polym. Sci. Polym. Phys. Ed.*, **23**, 205 (1985)
[14] C. M. Guttman, E. DiMarzio and J. D. Hoffman, *Polymer*, **22**, 1466 (1981)
[15] J. D. Hoffman and R. L. Miller, *Polymer*, **38**, 3151 (1997)
[16] V. B. F. Mathot, R. L. Scherrenberg and T. F. J. Pijpers, *Polymer*, **39**, 4541 (1998)
[17] M. Peeters, B. Goderis, C. Vonk, H. Reynaers and V. Mathot, *J. Polym. Sci., Part B: Polym. Phys.*, **35**, 2689 (1997)
[18] C. W. Bunn in "*Polythene*", Eds. A. Renfrew and P. Morgan, InterScience, New York, Chap. 7 (1957)
[19] G. T. Davis, J. J. Weeks, G. M. Martin and R. K. Eby, *J. Appl. Phys.*, **45**, 4175 (1974)
[20] C. M. Guttman, E. A. DiMarzio and J. D. Hoffman, *Polymer*, **22**, 1466 (1982)
[21] P. J. Flory, D. Y. Yoon and K. A. Dill, *Macromolecules*, **17**, 862 (1984)
[22] M. G. Broadhurst and F. I. Mopsik, *J. Chem. Phys.*, **54**, 4239 (1971)
[23] E. R. Walter and F. P. Reding, *J. Polym. Sci.*, **21**, 501 (1956)
[24] R. M. Eichhorn, *J. Polym. Sci.*, **31**, 197 (1958)
[25] P. R. Swan, *J. Polym. Sci.*, **56**, 409 (1962)
[26] C. H. Baker and L. Mandelkern, *Polymer*, **7**, 71 (1966)
[27] C. W. Bunn, "*Polyethylene*", Ed., A. Renfew and P. Morgan, Illife, London, Chap. 5
[28] P. W. Teare and D. R. Holmes, *J. Polym. Sci.*, **24**, 496 (1957)
[29] A. T. Jones, *J. Polym. Sci.*, **62**, 553 (1962)
[30] J. G. Fatou, C. H. Baker and L. Mandelkern, *Polymer*, **6**, 243 (1965)
[31] Y. Kikuchi and S. Krimm, *J. Macromol. Sci. - Phys.*, **B4(3)**, 461 (1970)
[32] K. Tanaka, T. Seto and T. Hara, *J. Phys. Soc. Japan*, **17**, 873 (1962)
[33] T. Seto, T. Hara and K. Tanaka, *Jap. J. Appl. Phys.*, **7**, 31 (1968)
[34] A. J. Pennings and A. Zwijnenburg, *J. Polym. Sci. Polym. Phys. Ed.*, **17**, 1011 (1979)
[35] N. A. J. M. van Aerle, P. J. Lemstra and A. W. M. Braam, *Polym. Commun.*, **30**, 7 (1989)
[36] D. C. Bassett, B. A. Khalifa and B. Turner, *Nature*, **239**, 106 (1972)
[37] M. Yasuniwa, C. Nakafuku and T. Takemura, *Polym. J.*, **4**, 526 (1973)
[38] S. Rastogi, M. Hikosaka, H. Kawabata and A. Keller, *Macromolecules*, **24**, 6384 (1991)
[39] K. Tashiro, S. Sasaki and M. Kobayashi, *Macromolecules*, **29**, 7460 (1996)
[40] G. Strobl, B. Ewen, E. W. Fischer and W. Piesczek, *J. Chem. Phys.*, **61**, 5257 (1974)
[41] M. Maroncelli, S. P. Qi, H. L. Strauss and R. G. Snyder, *J. Am. Chem. Soc.*, **104**, 6327 (1982)
[42] E. B. Sirota, H. E. King, Jr., D. M. Singer and H. H. Shao, *J. Chem. Phys.*, **98**, 5809 (1995)
[43] K. Tashiro, S. Sasaki, M. Kobayashi, Y. Izumi and K. Kobayashi, *Submitted to Macromolecules*
[44] P. J. Flory, *The J. Chem. Phys.*, **17**, 3, 223 (1949)
[45] P. J. Flory, *T. Faraday Soc.*, **51**, 848 (1955)